

^1H NMR Relaxation Study of Thermotropic Phase Transition in Poly(vinyl methyl ether)/D₂O Solutions

Jiří Spěváček,^{*,†,‡} Lenka Hanyková,[‡] and Larisa Starovoytova[‡]

Institute of Macromolecular Chemistry, Academy of Sciences of the Czech Republic, Heyrovsky Sq. 2, 162 06 Prague 6, Czech Republic, and Faculty of Mathematics and Physics, Charles University, V Holesovickach 2, 180 00 Prague 8, Czech Republic

Received July 2, 2004; Revised Manuscript Received July 30, 2004

ABSTRACT: ^1H NMR line shapes and spin–spin relaxation times T_2 have shown that in PVME/D₂O solutions the LCST transition results in limited mobility of most PVME units, evidently in connection with formation of compact globular-like structures. The minority mobile component, which does not take part in the phase transition, mostly consists of low-molecular-weight fraction of PVME, as shown by SEC. Measurements of spin–spin relaxation times of PVME methylene protons have shown that globular structures are more compact in dilute solutions in comparison with semidilute and concentrated solutions where globules contain a certain amount of water. A certain portion of water molecules bound at elevated temperatures in PVME globular structures in semidilute and concentrated solutions was revealed also from measurements of spin–spin and selective and nonselective spin–lattice relaxation times of residual HDO molecules. While the phase separation in dilute PVME solutions is associated with rapid dehydration of polymer chains, for semidilute and concentrated solutions T_2 measurements evidence that with time the originally bound water is slowly released from globular-like structures, and the character of the globules is changed from the spongelike to a rather compact one. From results obtained on D₂O solutions of PVME/poly(*N*-isopropylmethacrylamide) (PIPMAAm) mixtures it follows that this process is significantly slower for more rigid globular-like structures of PIPMAAm in comparison with globules of the flexible PVME.

Introduction

It is well-known that some acrylamide-based polymers and some other polymers, like poly(vinyl methyl ether) (PVME), in aqueous solution exhibit a lower critical solution temperature (LCST); i.e., they are soluble at low temperatures, but heating above the LCST results in phase separation. For PVME aqueous solutions the LCST is around 308 K,^{1–3} i.e., well above the temperature of the glass transition of PVME in bulk where values in the range $T_g = 191$ – 251 K are reported.⁴ On the molecular level, both phase separation in solutions and collapse transition in cross-linked hydrogels are assumed to be a macroscopic manifestation of a coil–globule transition followed by aggregation, as shown for acrylamide-based polymers in water by light scattering and small-angle neutron scattering.^{5–9} Contrary to acrylamide-based systems, the phase transition in both PVME/water solutions^{10–16} and radiation cross-linked PVME hydrogels^{11,15,17–19} was relatively little studied, and these studies are of recent date. Similarly to acrylamide-based polymers, the transition in PVME/water systems is probably associated with competition between hydrogen-bonding and hydrophobic interactions.^{10,14} The existence of molecular complex between water and PVME, which is stable at least up to a temperature close to the melting point of water¹¹ or to the transition temperature,¹⁰ has been shown by DSC, near-infrared, and viscometric measurements. In recent infrared spectroscopic study,¹³ Maeda has found that most of methyl groups of PVME are dehydrated

above the LCST, whereas there is only partial dehydration of the ether groups above the LCST.

Recently we used ^1H NMR spectroscopy to investigate changes in the dynamic structure during temperature-induced phase transition in PVME solutions and gels in a broad range of concentrations ($c = 0.1$ – 30 wt %) and cross-linking densities, respectively.^{12,15,16} For both linear and cross-linked systems, the phase transition is manifested by line broadening for a major part of PVME units, indicating the formation of more compact globular-like structures. While for dilute PVME solutions the transition as detected by NMR is virtually discontinuous, for semidilute and concentrated solutions and for concentrated swollen networks, the transition sets in at lower temperatures and is several kelvin broad. We also applied ^1H NMR to investigate phase transitions in D₂O solutions of poly(*N*-isopropylmethacrylamide) (PIPMAAm)²⁰ and PVME/PIPMAAm mixtures.²¹

In the present study we investigated the thermotropic phase transition in PVME/D₂O systems by ^1H NMR relaxation methods. Both measurements of line widths and spin–spin relaxation times T_2 of PVME protons and measurements of spin–spin relaxation times and selective (SE) and nonselective (NS) spin–lattice relaxation times T_1 of water (HDO) molecules were employed to this purpose. T_2 measurements of HDO were done also on D₂O solutions of PVME/PIPMAAm mixtures to compare behavior for globular-like structures formed by flexible PVME chains with rather rigid PIPMAAm globular structures. (For PIPMAAm the LCST ≈ 315 K is well below the respective $T_g = 449$ K.²²)

Experimental Section

Samples. Linear PVME (purchased from Aldrich, supplied as 50 wt % aqueous solution; molecular weight determined by

[†] Academy of Sciences of the Czech Republic.

[‡] Charles University.

* Corresponding author: Tel +420-296-809-380; Fax +420-296-809-410; e-mail spevacek@imc.cas.cz.

SEC in THF: $M_w = 60\,500$, $M_w/M_n \approx 3$; tacticity by ^1H NMR: 59% of isotactic diads¹⁵) was used after drying to prepare PVME/D₂O (99.9% of deuterium) solutions of desired concentration in the range $c = 0.1$ –60 wt %. Cross-linked PVME/D₂O sample was prepared by γ -irradiation of the PVME/D₂O solution ($c = 10$ wt %) (^{60}Co γ -source with a dose rate of 0.8 kGy/h, Artim Prague); radiation dose was $\gamma = 20$ kGy and shear modulus $G = 27$ g/cm². PIPMAAm was prepared by polymerization of IPMAAm monomer in an ethanol/water mixture initiated by 4,4'-azobis(4-cyanopentanoic acid); the volume fraction of monomer in the mixture was 0.25. All PVME/D₂O and PVME/PIPMAAm/D₂O samples in 5 mm NMR tubes were degassed and sealed under argon; sodium 2,2-dimethyl-2-silapentane-5-sulfonate (DSS) was used as an internal NMR standard.

NMR Measurements. High-resolution ^1H NMR spectra were recorded with a Bruker Avance 500 spectrometer operating at 500.1 MHz. Typical measurement conditions were as follows: 90° pulse width 12 μs , relaxation delay 10 s, spectral width 4735 Hz, acquisition time 1.73 s, 16 scans. To detect correctly broad lines, spectra with spectral width 15 015 Hz were also measured. The ^1H spin–spin relaxation times T_2 were measured using the same instrument and the CPMG²³ pulse sequence $90^\circ_x - (t_d - 180^\circ_y - t_d)_n$ –acquisition for polymer protons with $t_d = 0.5$ ms (at 305 K or at lower temperature) or 0.15 ms (0.12 ms in some cases) (at 309.5 K). The total time for T_2 relaxation was an array of ~ 60 values varying from 0.26 ms to 5 s. Every experiment was done with eight scans (64 scans for dilute solutions; in measurements of time dependences of T_2 , 16 scans were done for dilute solutions to minimize the duration of the experiment), relaxation delay of 10 s, spectral width 10 kHz, and acquisition time of 0.82 s. Integrated intensities of CH (separately for *mr* and *mm* triads), CH₃, and CH₂ (separately for low-field proton of *m*-diads and for high-field proton of *m*-diads and both protons of *r*-diads) resonances were used for T_2 analysis at temperatures below the transition (305 and 298 K). Above the transition (at 309.5 K), due to existence of the broad component, only the integrated intensities of the composite CHOCH₃ band and composite CH₂ band could be used for the analysis. T_2 measurements of the solvent (residual HDO) were done using the CPMG pulse sequence with $t_d = 5$ ms, relaxation delay 80–100 s, and eight scans; other parameters were the same as specified above. T_2 values (and in the case of spin–spin relaxation of PVME protons also intensities of respective components) as appear in Tables 1, 2, and 4 represent an average values obtained from two independent measurements. The relative error for T_2 values of PVME and HDO protons did not exceed $\pm 8\%$ and $\pm 5\%$, respectively. Selective and nonselective spin–lattice relaxation times T_1 of HDO were measured using an inversion recovery pulse sequence $180^\circ - \tau - 90^\circ$ with eight scans separated by a relaxation delay of 80–200 s; 15–20 τ values were used. In selective T_1 measurements, the Gaussian-shaped pulse²⁴ was used to generate selectively the first 180° pulse. For $c = 6$ wt % and several temperatures, a good reproducibility was found from three independent T_1 measurements. Some spectra were also recorded with a Bruker DPX 300 spectrometer operating at 300.1 MHz to obtain line widths of the broad component at another frequency. In all measurements the temperature was maintained constant within ± 0.2 K with a BVT 3000 temperature unit.

Size Exclusion Chromatography (SEC). A modular liquid chromatograph (Laboratory Instruments, Czech Republic) equipped with refractometric and UV detectors and a separation column PL Mixed B (Polymer Laboratories, UK) with THF as a mobile phase was used for molecular weight determination. Calibration was performed with polystyrene standards (Merck).

Results and Discussion

^1H NMR Spectra and SEC Analysis. High-resolution ^1H NMR spectra of PVME/D₂O solution ($c = 4$ wt %) measured at two slightly different temperatures (307

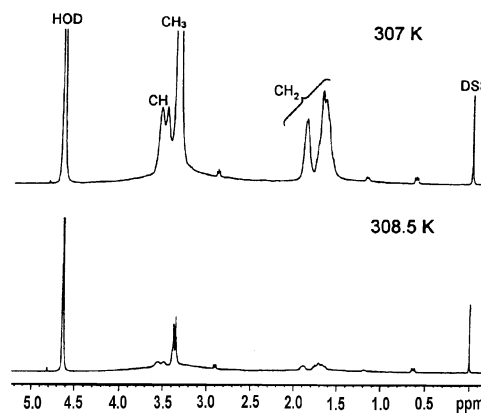


Figure 1. 500.1 MHz ^1H NMR spectra of PVME/D₂O solution ($c = 4$ wt %) measured at 307 and 308.5 K under the same instrumental conditions.¹⁵

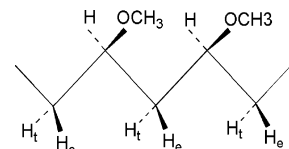


Figure 2. Schematic representation of isotactic diad of PVME in the trans–trans conformation of the main chain.

and 308.5 K) and under identical instrument conditions are shown in Figure 1. The assignment of resonances to various types of protons of PVME and to residual water (HDO) is shown in spectrum measured at 307 K. The splitting of CH, CH₃, and CH₂ resonances of PVME is due to tacticity.^{25,26} For CH protons, two resolved lines correspond to heterotactic *mr* (low-field line) and isotactic *mm* (high-field line) triads. For CH₂ region, the line at 1.9 ppm corresponds to one proton from *m*-diads while the other proton of *m*-diads and both CH₂ protons of *r*-diads contribute to the composite band at 1.7 ppm (the latter band also overlaps with weak multiplet from DSS standard). In the *m*-diad of PVME in trans–trans conformation (preferred conformation for the isotactic chain^{27,28}) (Figure 2), the CH₂ proton which projects on the same side as the ester groups (i.e., which is syn to the ester group) is designated as erythro (e), the other CH₂ proton (anti to the ester groups) being threo (t). For 1,1,3-diethoxybutane, a dimer model of poly(vinyl ethyl ether),²⁹ as well as for acrylates and poly(methyl methacrylate) (PMMA),^{30,31} it has been shown that downfield CH₂ resonance corresponds to e-CH₂ protons, and therefore it can be assumed that this holds also for CH₂ line from *m*-diads of PVME at 1.9 ppm (cf. Figure 1).

While an ordinary spectrum of the polymer in solution was recorded at 307 K, with line widths of the order of ~ 10 Hz, the most significant effect observed at higher temperature (308.5 K) is a marked decrease in the integrated intensity of all PVME lines. This is evidently due to the fact that at temperature above the LCST the mobility of most PVME units is reduced to such an extent that corresponding lines became too broad to be detected in high-resolution spectra. Figure 3 shows ^1H NMR spectra of PVME/D₂O solution ($c = 2$ wt %) measured at 312 K with larger spectral width and higher amplification. A typical two-component line shape can be seen. Most of PVME units contribute to the broad component on which narrow lines of PVME units retaining a high mobility are superimposed (sharp peaks at 0.62, 1.75, and 2.9 ppm correspond to DSS

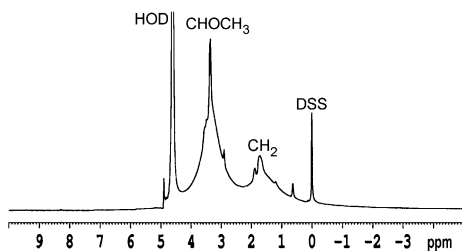


Figure 3. 500.1 MHz ^1H NMR spectrum of PVME/ D_2O solution ($c = 2$ wt %) measured at 312 K with spectral width 15 kHz.

standard). Similar behavior as shown in Figures 1 and 3 was found also for other polymer concentrations. All studied solutions exhibit a milk-white opalescence at 308.5 K and higher temperatures, so corroborating that a marked line broadening of a major part of PVME units is due to the phase separation and formation of compact globular-like structures.

In addition to the broad component, a small narrow PVME component is visible in the spectra at 308.5 K and other temperatures above LCST. From the comparison of absolute integrated intensities,¹⁵ it follows that the fraction of phase-separated PVME segments is ~ 0.85 . One can speculate about the nature of PVME segments which contribute to the minority mobile component. A possible explanation might be that mobile PVME units are those on the surface of globular-like particles or segments connecting globules in "pearl necklace model" which recently has been shown consistent with NMR spectra of polyelectrolytes in poor solvents.³² However, for other phase-separated systems that show similar globular-like structures, like D_2O solutions of PIPAAm, poly(*N*-isopropylacrylamide) (PIPAAm), and poly(*N,N*-diethylacrylamide) above the respective LCST, the fraction of phase-separated polymer segments found from NMR measurements is equal to 1 or close to 1; i.e., virtually no narrow lines were detected in these cases.^{20,21,33,34} Therefore, as the most probable explanation for 15% of PVME segments that contribute to minority narrow (mobile) component and do not participate in phase separation, we suggested^{12,15} that they probably are from a low-molecular-weight fraction which one can expect for polymer with rather large polydispersity ($M_w/M_n \cong 3$), as in our case. To support this hypothesis, the following experiment was done. PVME/ H_2O solution ($c = 6$ wt %) was centrifuged for ~ 10 min at 313 K (ultracentrifuge Beckman L8 55, rotor SW28/E, 15 000 rpm). After seclusion of the phase-separated part the remaining solution was analyzed by ^1H NMR and found that it still contains a small amount of PVME. This solution was dried and subsequently analyzed by SEC with THF as a mobile phase. The respective SEC eluogram is shown in Figure 4. From this figure it follows that really only low-molecular-weight fraction of PVME is present in water solution after removal of the phase-separated polymer. There are several peaks visible on SEC curve, and comparison with polystyrene standards shows that PVME oligomers (6–10-mers) are prevailing in the analyzed sample. One can assume that a certain minimum chain length is a prerequisite for the phase separation as a consequence of the cooperative character of the respective interactions. On the basis of Figure 4, one can assume that for PVME in aqueous solution such minimum chain length amounts on average ~ 10 monomeric units; however, this figure also shows that some

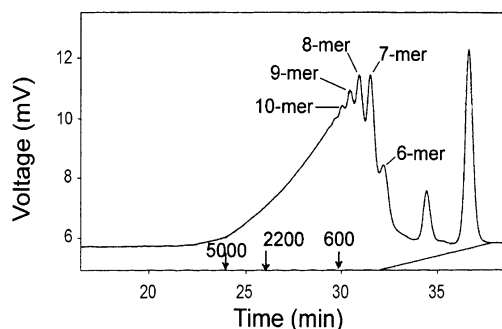


Figure 4. SEC curve (in THF) of the PVME remaining in aqueous solution after seclusion the phase separated part by centrifugation at 313 K and 15 000 rpm (polystyrene standards are shown by arrows).

chains with degree of polymerization up to ~ 50 are not phase-separated at 313 K.

Spin–Spin Relaxation Times of PVME Protons.

T_2 relaxation curves of various types of PVME protons in PVME/ D_2O solution at 298 K are shown in Figure 5. We have found that at temperatures below the transition (298 and 305 K) the spin–spin relaxation of all proton types of PVME was biexponential. The T_2 values together with intensities of both components (in parentheses) as obtained at 305 K for all five resolved bands of PVME protons (CH from heterotactic (*mr*) and isotactic (*mm*) triads, OCH_3 , CH_2 e-protons from *m*-diads and composite band from t- CH_2 protons of *m*-diads, and both CH_2 protons of *r*-diads) are summarized for several concentrations of the solution in Table 1. T_2 values and intensities of the components obtained at 298 K were similar. The biexponential ^1H spin–spin relaxation was recently observed for polyacrylamide in D_2O solution³⁵ and for PMMA in some organic solvents.³⁶ Similarly, as authors of the cited papers, we assigned the shorter and longer T_2 components of PVME protons to polymer segments affected by polymer–polymer and polymer–solvent interactions, respectively.

From Table 1 it follows that T_2 values of both components virtually do not depend on the polymer concentration. Somewhat longer values of long component of T_2 found for composite (*m*(*t*) + *r*) CH_2 band in dilute solutions ($c = 0.1$ and 0.2 wt %) might be partly due to the fact that in dilute solutions a weak signal from DSS (which also contributes to this band) cannot be neglected. Also, intensities of both components are concentration-independent, with one exception: for e- CH_2 protons in *m*-diads the intensity of the short T_2 component significantly decreases with decreasing polymer concentration (Table 1). This result might indicate that these e- CH_2 protons are most affected by water molecules. Assuming that water forms hydrogen bonds with oxygen atoms of PVME, it follows from Figure 2 that e- CH_2 protons in *m*-diads (in preferred trans–trans conformation) are on the same side of the chain as oxygens. For other PVME protons, the intensity of the short T_2 component is quite large even for dilute solutions, indicating rather intramolecular origin of this component. Table 1 also shows that intensities of both components depend on the stereochemical configuration (tacticity). For CH protons, the intensity of the long T_2 component is significantly higher for *mm*-triads as compared with *mr*-triads. Similarly, for dilute solutions this holds also for e- CH_2 protons from *m*-diads in comparison with mixed CH_2 band from t-protons of *m*-diads and both protons of *r*-diads. This indicates that

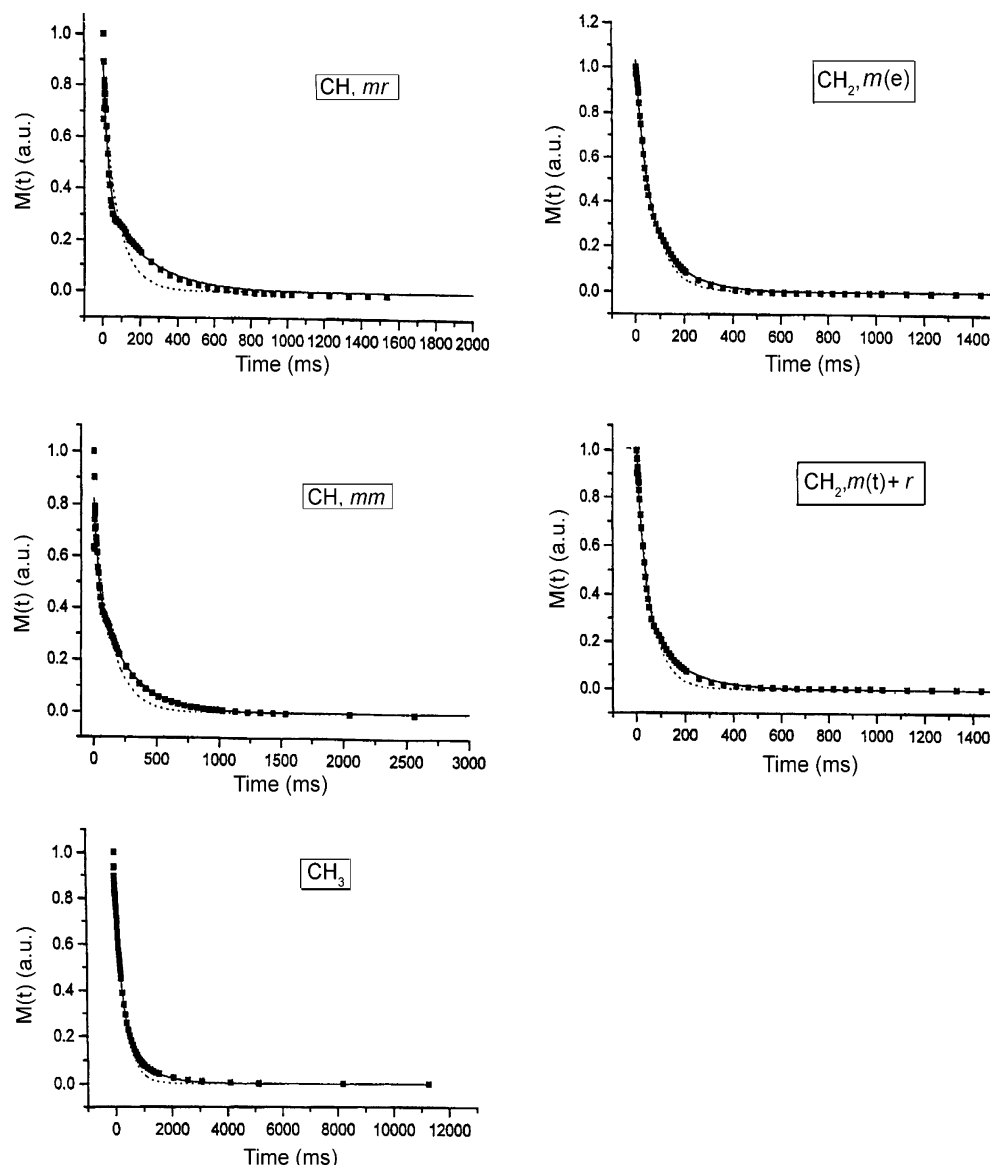


Figure 5. T_2 relaxation curves of various types of PVME protons in PVME/D₂O solution ($c = 2$ wt %) measured at 298 K. Full lines show two-exponential fit, dotted lines show a single-exponential fit.

Table 1. Spin-Spin Relaxation Times T_2 and Intensities of Respective Components (in Parentheses) of PVME Protons for PVME/D₂O Solutions at 305 K

c (wt %)	T_2 (ms)				
	OCH		OCH ₃	CH ₂	
	mr	mm		$m(e)$	$m(t) + r$
0.1	164 (25%)	176 (49%)	807 (33%)	117 (62%)	312 (33%)
	21 (75%)	21 (51%)	252 (67%)	27 (37%)	37 (67%)
0.2	222 (29%)	229 (49%)	725 (42%)	138 (53%)	370 (30%)
	23 (71%)	26 (51%)	235 (58%)	32 (47%)	37 (70%)
2	211 (37%)	223 (55%)	733 (49%)	189 (30%)	268 (22%)
	24 (63%)	27 (45%)	196 (51%)	42 (70%)	35 (78%)
6	237 (30%)	199 (49%)	572 (47%)	154 (29%)	132 (33%)
	23 (70%)	23 (51%)	144 (53%)	35 (71%)	28 (67%)

polymer–solvent interactions are preferred for isotactic sequences (m -diads or mm -triads) or, in another words, that polymer–polymer interactions prevail for sequences containing r -diads.

At temperatures above the transition (309.5 K), the T_2 relaxation of PVME protons (with spectra measured in analogous way to that in Figure 3) was triexponential. In addition to two components observed below the transition, a predominant, very short component was

found ($T_2 < 1$ ms), which is clearly visible in Figure 6. The T_2 values and intensities of three T_2 components are for several concentrations of solutions summarized in Table 2. From Table 2 it follows that intensities of the shortest T_2 component do not depend on the concentration of the solution and amount on average $\sim 75\%$. This value agrees well with the phase-separated fraction $p = 0.85$ as determined from integrated intensities of high-resolution ¹H NMR spectra¹⁵ and confirms that shortest T_2 component corresponds to PVME segments forming globular-like structures. Very long T_2 values of the longest component as obtained for $c = 0.1$ wt % are again due to DSS (weak multiplets of DSS contribute to both CHOCH₃ and CH₂ broad bands). While T_2 values of the shortest component of CHOCH₃ protons virtually do not depend on the polymer concentration, for CH₂ protons the very short component decreases with decreasing concentration of the solution (Figure 7). This shows that globular-like structures are more compact in dilute solution in comparison with semidilute or concentrated solutions, where globules probably contain a certain amount of water. The fact

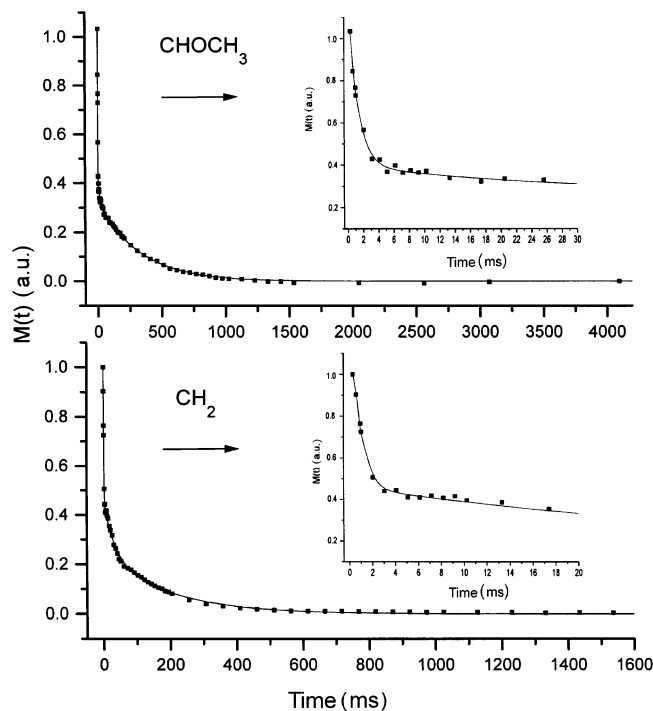


Figure 6. T_2 relaxation curves of CHOCH_3 and CH_2 PVME protons in PVME/ D_2O solution ($c = 2$ wt %) measured at 309.5 K. The inset shows in detail the beginning of the curve.

Table 2. Spin-Spin Relaxation Times T_2 and Intensities of Respective Components (in Parentheses) of PVME Protons for PVME/ D_2O Solutions at 309.5 K

c (wt %)	T_2 (ms)	
	CHOCH_3	CH_2
0.1	5515 ^a (14%)	3040 ^a (11%)
	362 (11%)	126 (18%)
	0.92 (75%)	0.30 (71%)
0.2	506 (27%)	425 (16%)
	32.9 (11%)	33.4 (28%)
	0.81 (62%)	0.43 (56%)
2	399 (17%)	187 (9%)
	25.8 (6%)	29.6 (12%)
	0.87 (77%)	0.54 (79%)
6	679 (9%)	470 (5%)
	29.9 (8%)	38.5 (10%)
	0.91 (83%)	0.72 (85%)

^a Values probably affected by DSS.

that T_2 values of the short component of CHOCH_3 protons (with dominant contribution of CH_3 protons) do not depend on the concentration of the solution is in accord with result of Maeda,¹³ who has found by infrared spectroscopy that at temperatures above the LCST most methyl groups of PVME are dehydrated.

It is well-known that assuming a Lorentzian line shape there is a simple relation between line width $\Delta\nu$ and spin–spin relaxation time T_2 :

$$\Delta\nu = (\pi T_2)^{-1} \quad (1)$$

In Table 3, the line widths $\Delta\nu_{\text{meas}}$ measured for broad CHOCH_3 and CH_2 bands, corresponding to the phase-separated PVME units, are compared with values obtained using T_2 values of the shortest T_2 -component and eq 1. Similarly to T_2 values, also measured line widths of CHOCH_3 band do not depend on the concentration of the solution, while line widths $\Delta\nu_{\text{meas}}$ of CH_2 protons increase with decreasing concentration of the

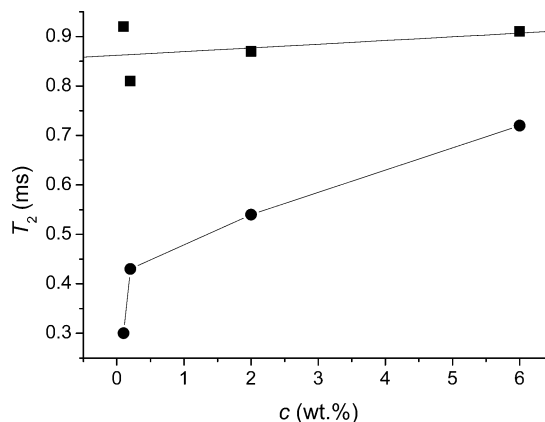


Figure 7. Concentration dependence of a very short component of spin–spin relaxation time T_2 as determined for CHOCH_3 (■) and CH_2 (●) protons in PVME/ D_2O solutions.

Table 3. Comparison of Measured Line Widths $\Delta\nu_{\text{meas}}$ and Line widths Calculated from T_2 Values Using the Relation $\Delta\nu_{\text{calc}} = (\pi T_2)^{-1}$ for the Broad Component of PVME Protons in PVME/ D_2O Solutions of Various Concentration at 309.5 K

c (wt %)	CHOCH_3		CH_2	
	$\Delta\nu_{\text{meas}}$ (Hz)	$\Delta\nu_{\text{calc}}$ (Hz)	$\Delta\nu_{\text{meas}}$ (Hz)	$\Delta\nu_{\text{calc}}$ (Hz)
0.1	444	346	946	1060
0.2	410	449	752	740
2	408	366	734	590
6	427	350	728	440

solution. While the measured line widths $\Delta\nu_{\text{meas}}$ and line widths calculated from measured T_2 values (using eq 1) are in mutual agreement for CHOCH_3 protons (for all concentrations) and also for CH_2 protons (for dilute solutions), especially taking into account that both broad lines are composed of two components with chemical shifts that differ by approximately 0.2 ppm (i.e., by approximately 100 Hz in frequency scale), for $c = 6$ wt % the difference 288 Hz found between $\Delta\nu_{\text{meas}}$ and $\Delta\nu_{\text{calc}}$ values is significantly larger. Probably, in this solution a dispersion of chemical shifts of CH_2 protons of PVME, as consequence of the bound water molecules, contributes to the line broadening. This conclusion is also corroborated by the fact that for $c = 6$ wt % the line width 560 Hz, as determined for PVME CH_2 protons at frequency 300.1 MHz and temperature 309.5 K, is smaller in comparison with the line width 728 Hz found at 500.1 MHz (cf. Table 3).

Spin–Spin Relaxation Times T_2 and Selective and Nonselective Spin–Lattice Relaxation Times T_1 of HDO. To characterize polymer–solvent interactions in PVME/ D_2O solutions, we used measurements of ^1H spin–spin relaxation times T_2 and selective (SE) and nonselective (NS) ^1H spin–lattice relaxation times T_1 of residual HDO molecules. The T_2 values of HDO molecules in solutions of various polymer concentration and measured at temperatures below (305 K) and above (309.5 K) the transition are shown in Table 4. Although all samples were degassed in the same way, T_2 values at 305 K seem to be somewhat scattered, and therefore the ratio $r = (T_2(309.5)/T_2(305))$ is probably more appropriate to compare the samples of different polymer concentration. While for dilute solutions ($c = 0.1$ and 0.2 wt %) T_2 values measured at 305 and 309.5 K did not differ too much ($r = 0.74$ – 0.80), a significant difference was found for higher concentrations where T_2 values at 309.5 K were 1 order of magnitude shorter

Table 4. ¹H Spin–Spin Relaxation Times T_2 of HDO Molecules in PVME/D₂O Solutions at 305 and 309.5 K

c (wt %)	T_2 (s)		r^a
	305 K	309.5 K	
0.1	4.2	3.1	0.74
0.2	5.4	4.3	0.80
2	8.7	1.5	0.17
6	4.8	0.44	0.09
10	4.5	0.74	0.16

$$^a r = T_2(309.5)/T_2(305).$$

than those at 305 K ($r = 0.09$ – 0.17). This shows that in semidilute and concentrated PVME solutions at temperature above the transition there is a portion of HDO molecules that exhibit a lower (spatially restricted) mobility, similarly to the phase-separated PVME. Evidently, this portion corresponds to HDO molecules bound in globular-like structures. In all cases the T_2 relaxation curves were exponential, indicating a fast exchange between bound and free sites regarding T_2 values (~ 1 s); i.e., the lifetime of the bound HDO molecules is ≤ 0.1 s. In such case the observed relaxation time $T_{2\text{obs}}$ is given as

$$(T_{2\text{obs}})^{-1} = (1 - f)(T_{2F})^{-1} + f(T_{2B})^{-1} \quad (2)$$

where subscripts F and B correspond to free and bound states, respectively, and f is the fraction of bound HDO molecules. In accord with results of T_2 measurements for PVME protons, it follows from Table 4 that in dilute solutions the fraction of bound HDO molecules is almost negligible.

Another approach that we have used is based on measurements of selective (SE) and nonselective (NS) ¹H spin–lattice relaxation times T_1 of residual HDO.³⁷ Previously, we have found this approach as very effective in studies of polymer–solvent interactions in thermoreversible polymer gels.^{38–42} Assuming a dipolar relaxation mechanism, for any proton i its nonselective and selective relaxation rates are given by³⁷

$$(T_1)^{-1}(\text{NS}) = \sum \rho_{ij} + \sum \sigma_{ij} \quad (3)$$

$$(T_1)^{-1}(\text{SE}) = \sum \rho_{ij} \quad (4)$$

In these equations, ρ_{ij} and σ_{ij} are the direct relaxation term and the cross-relaxation term, respectively. For a pair of protons i and j

$$\rho_{ij} = (\hbar^2 \gamma_H^4 / 10 r_{ij}^6) \{ 3\tau_c / [1 + (\omega_0 \tau_c)^2] + 6\tau_c / [1 + 4(\omega_0 \tau_c)^2] + \tau_c \} \quad (5)$$

$$\sigma_{ij} = (\hbar^2 \gamma_H^4 / 10 r_{ij}^6) \{ 6\tau_c / [1 + 4(\omega_0 \tau_c)^2] - \tau_c \} \quad (6)$$

where r_{ij} is the interproton distance, ω_0 is the resonance frequency, τ_c is the motional correlation time, and other constants have their usual meanings. From eqs 3–6 it follows that a marked difference exists for relaxation times $T_1(\text{SE})$ and $T_1(\text{NS})$ for correlation times $\tau_c > \omega_0^{-1}$; for the ratio $T_1(\text{SE})/T_1(\text{NS})$ the limiting values are 1.5 for $\omega_0 \tau_c \ll 1$ and 0 for $\omega_0 \tau_c \gg 1$.

We measured temperature dependences of ¹H $T_1(\text{NS})$ and $T_1(\text{SE})$ relaxation times for HDO molecules in PVME/D₂O solutions of variable polymer concentration. In all cases the relaxation curves were exponential. The results obtained for $c = 6$ wt % (a) and $c = 60$ wt % (b)

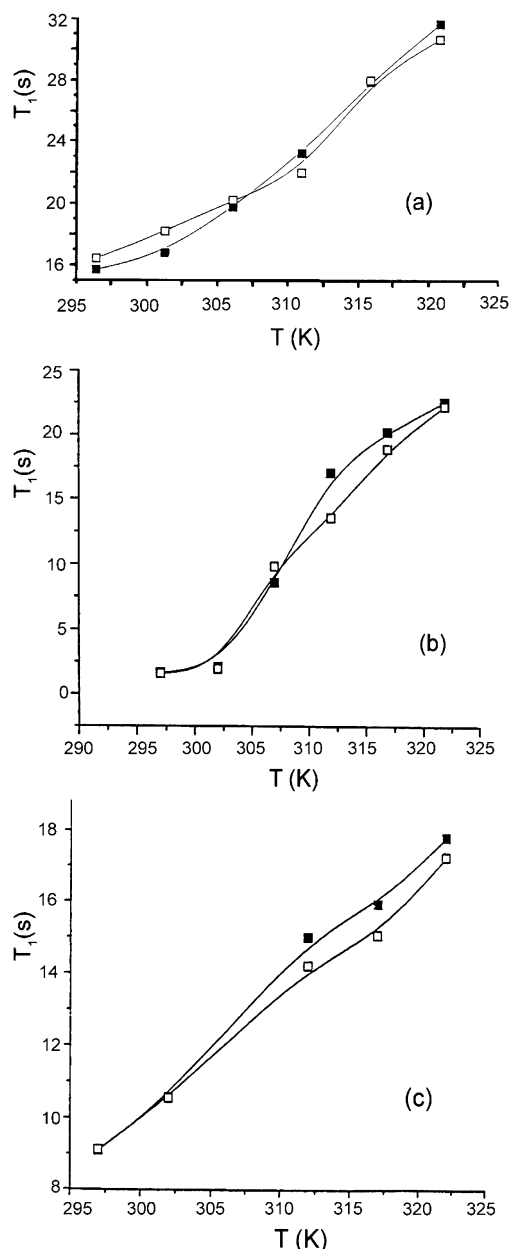


Figure 8. Selective (open symbols) and nonselective (filled symbols) ¹H spin–lattice relaxation times T_1 (standard deviation less than 0.5%) of HDO molecules in PVME/D₂O solutions (a, b) and PVME/D₂O swollen network (c) as a function of temperature at 500.1 MHz; $c = 6$ (a), 60 (b), and 10 wt % (c).

as well as for swollen PVME/D₂O gel ($c = 10$ wt %) obtained by radiation cross-linking (c) are shown in Figure 8. Similar temperature dependences of $T_1(\text{NS})$ and $T_1(\text{SE})$ as shown in Figure 8a for $c = 6$ wt % were also found for somewhat lower ($c = 4$ wt %) or higher ($c = 10$ wt %) concentrations. Figure 8 shows that both $T_1(\text{SE})$ and $T_1(\text{NS})$ values monotonically increase with increasing temperature; we did not observe a decrease of $T_1(\text{NS})$ values at the transition region, as found for water protons in PIPAAm aqueous solutions⁴³ or for HDO in PIPMAAm/D₂O solutions,⁴⁴ probably in connection with relatively high mobility of PVME segments even in globular-like structures. However, from Figure 8 it follows that while at temperatures below the transition ($T \leq 307$ K) $T_1(\text{NS})$ values are somewhat lower in comparison with $T_1(\text{SE})$ (for $c = 4, 6$, and 10 wt %), as expected for $\omega_0 \tau_c < 1$, or $T_1(\text{NS})$ and $T_1(\text{SE})$ values are virtually identical (for $c = 60$ wt % and for

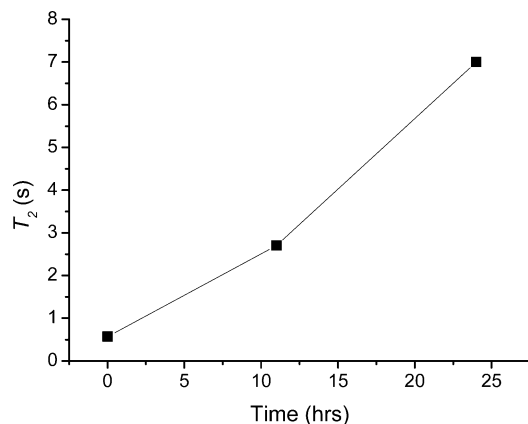


Figure 9. Time dependence of spin–spin relaxation times T_2 for HDO protons in PVME/D₂O solution; $c = 6$ wt %.

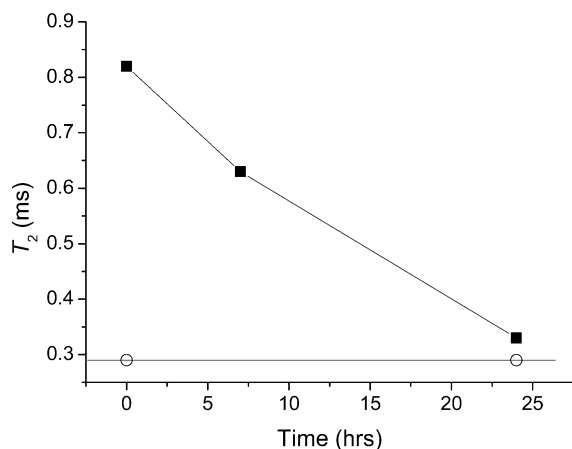


Figure 10. Time dependences of spin–spin relaxation times T_2 for CH₂ protons of PVME in PVME/D₂O solutions; $c = 0.1$ wt % (open symbols) and 6 wt % (filled symbols).

the swollen network), as expected for $\omega_0\tau_c \approx 1$, at temperatures above the LCST transition $T_1(\text{NS}) > T_1(\text{SE})$; i.e., the cross-relaxation term $\sum \sigma_{ij}$ in eq 3 has to be negative. For dilute PVME/D₂O solution ($c = 0.2$ wt %) the behavior shown in Figure 8 was not found. These results confirm that in semidilute and concentrated solutions (and gels) at elevated temperatures, where most PVME forms globular-like structures, a portion of HDO molecules are bound in these structures. These HDO molecules exhibit a slow-motion behavior ($\omega_0\tau_c > 1$) because their motion is spatially anisotropic, with fast exchange between bound and free sites (cf. expression analogous to eq 2).

Time Dependences of the Spin–Spin Relaxation Times T_2 . We were interested in knowing whether the amount of water bound in PVME globular structures formed in semidilute and concentrated aqueous solutions, as revealed from T_2 measurements of residual HDO (resulting in 1 order of magnitude shorter T_2 values in comparison with a few kelvin lower temperature below the transition) and from T_2 measurements of CH₂ protons of PVME (resulting in longer T_2 values of a very short component in comparison with dilute solutions) is changing with time or not. The sample was kept for all the time in the magnet of NMR spectrometer at desired temperature (309.5 K). Figures 9 and 10 show the time dependence of relaxation time T_2 of HDO molecules and time dependences of a very short component of relaxation time T_2 as determined for CH₂

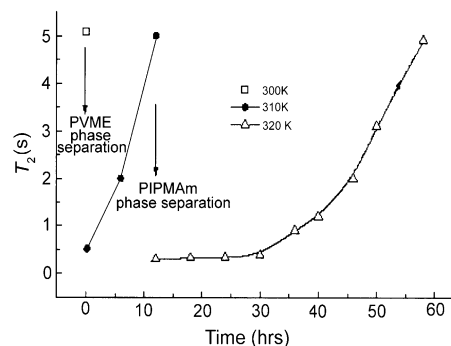


Figure 11. Time dependence of spin–spin relaxation times T_2 of HDO in D₂O solutions of PVME/PIPMAAm mixtures (molar ratio of monomeric units 3/1, $c = 5$ wt %) at 310 and 320 K.

protons of PVME, respectively, both measured at 309.5 K.

While for $c = 0.1$ wt %, T_2 values of HDO obtained after 24 h ($T_2 = 4$ s) only slightly differ from the respective value in Table 4; for $c = 6$ wt % it follows from Figure 9 that T_2 values of HDO very slowly increase with time, reaching after 24 h a similar value as observed at temperature below the transition (cf. Table 4). Simultaneously, for $c = 6$ wt % values of a very short T_2 component of CH₂ protons of PVME (Figure 10) slowly decrease with time, reaching after 24 h a similar value as found for dilute solution ($c = 0.1$ wt %). Even after very long time (\sim day) we did not observe any sedimentation of the phase-separated part in the studied sample. Therefore, these results evidence that water, originally bound in globular-like structures, is with time very slowly released from these structures; this process takes ~ 24 h.

To compare this behavior, as found for globular structures formed by flexible PVME (LCST temperature is for PVME at least 60 K above the T_g of PVME in bulk⁴), with other system where globular-like structures are more rigid (in the glassy state), we have done similar T_2 measurements for HDO molecules in D₂O solutions of PVME/PIPMAAm mixtures (molar composition of respective monomeric units 3/1; $c = 5$ wt %). As we have shown recently, there are two phase transitions in these mixtures at temperatures roughly corresponding to LCSTs of neat PVME and PIPMAAm (308 and 315 K, respectively).²¹ From temperature dependences of T_2 of residual HDO in D₂O solutions of PVME/PIPMAAm mixtures it further follows that a certain portion of water is bound both to globular-like structures of PVME and PIPMAAm components, in relative amounts depending on the composition of the mixture. In the experiment described in Figure 11, temperature was first increased from 300 to 310 K, i.e., above the transition temperature of PVME but below the PIPMAAm transition. Then time dependence of T_2 was followed at this temperature. After initial drop, T_2 values slowly increased with time, similarly as shown in Figure 9, and after 12 h a similar T_2 value was reached as was originally at 300 K. Then temperature was increased to 320 K, i.e., above the transition temperature of PIPMAAm. T_2 values of HDO molecules again first dropped and then after ~ 20 h very slowly increased with time, again showing a release of water, in this case from PIPMAAm globular-like structures. Figure 11 demonstrates that this releasing process is for more rigid globular structures of PIPMAAm about

4 times slower as compared with globular structures formed by flexible PVME segments.

The following picture concerning globular-like structures can be deduced from spin–spin and spin–lattice relaxation measurements, including time dependences. Interchain interactions are important for globular-like structures formed in semidilute and concentrated solutions. The globules probably exhibit a spongelike structure, containing pores where molecules of water can be accommodated; such bound water molecules can exchange fast with surrounding bulk water. With time the bound water is slowly squeezed out by polymer segments, pores disappear, and globules become rather compact. In contrast to this behavior, in dilute solutions globular-like structures are rather compact and dehydrated already immediately after phase transition (they are mostly formed by single macromolecules).

Conclusions

¹H NMR spectral line shapes have shown that temperature-induced phase separation in PVME/D₂O solutions results in a marked line broadening of a major part of polymer segments, evidently due to the formation of rather compact globular-like structures. The minority (~15%) mobile component, which does not participate in the phase separation, comes mostly from PVME oligomers (~10-mers), as shown by SEC. At temperatures below the LCST transition (298 and 305 K), the spin–spin relaxation of all proton types of PVME was biexponential, with shorter and longer components assigned to polymer segments affected by polymer–polymer and polymer–solvent interactions, respectively. The intensities of both components depend on the stereochemical configuration (tacticity). The concentration dependence of intensities of both components found for erythro-CH₂ protons in isotactic diads indicates that these protons are most affected by water molecules. Measurements of spin–spin relaxation time T_2 in PVME/D₂O solutions at temperature above the transition (309.5 K) have shown that a very short component ($T_2 < 1$ ms) dominates the spin–spin relaxation of PVME protons. For CHOCH₃ protons, T_2 values of a very short component do not depend on the concentration of the solution, in accord with infrared results¹³ showing that most methyl groups of PVME are dehydrated above the LCST. For CH₂ protons, T_2 values of a very short component decrease with decreasing concentration of solutions, showing that globular-like structures are more compact in dilute solutions, compared with semidilute or concentrated solutions, where globules probably contain a certain amount of water. This is in accord with measurements of spin–spin relaxation time T_2 and selective and nonselective spin–lattice relaxation times T_1 of residual HDO which evidenced that for semidilute and concentrated solutions (and gels) above LCST, a part of HDO molecules is bound in PVME globular structures. T_2 measurements (on residual HDO and on CH₂ protons of PVME) also show that with time the originally bound water is very slowly squeezed out from globular-like structures existing in semidilute and concentrated solutions, and the character of these globules is changed from the spongelike to rather compact one. On the contrary, dehydration of PVME chains is rapid in dilute solutions. From results obtained on D₂O solutions of PVME/PIPMAAm mixtures ($c = 5$ wt %) it follows that the water releasing process is significantly slower for more rigid globular-

like structures of PIPMAAm component (at temperatures well below the T_g of PIPMAAm in bulk) in comparison with globules of the flexible PVME component (at temperatures well above the respective T_g).

Acknowledgment. This work was supported by the Grant Agency of the Academy of Sciences of the Czech Republic (Project IAA4050209) and the Grant Agency of the Charles University (Grant 294/2004/B). The authors thank Dr. P. Holler for SEC analysis.

References and Notes

- (1) Molyneux, P. *Water-Soluble Synthetic Polymers: Properties and Behavior*; CRC Press: Boca Raton, FL, 1983; Vol. 1, pp 58–61.
- (2) Horne, R. A.; Almeida, J. P.; Day, A. F.; Yu, N.-T. *J. Colloid Interface Sci.* **1971**, *35*, 77–84.
- (3) Schafer-Soenen, H.; Moerkerke, R.; Berghmans, H.; Koningsveld, R.; Dušek, K.; Šolc, K. *Macromolecules* **1997**, *30*, 410–416.
- (4) Andrews, R. J.; Grulke, E. A. In Brandrup, J., Immergut, E. H., Grulke, E. A., Eds.; *Polymer Handbook*, 4th ed.; Wiley: New York, 1999; p VI-201.
- (5) Fujishige, S.; Kubota, K.; Ando, I. *J. Phys. Chem.* **1989**, *93*, 3311–3313.
- (6) Kubota, K.; Fujishige, S.; Ando, I. *J. Phys. Chem.* **1990**, *94*, 5154–5158.
- (7) Zhu, P. W.; Napper, D. H. *Macromol. Chem. Phys.* **1999**, *200*, 1950–1956.
- (8) Wang, X.; Wu, C. *Macromolecules* **1999**, *32*, 4299–4301.
- (9) Pleštil, J.; Ostanevich, Y. M.; Borbely, S.; Stejskal, J.; Ilavský, M. *Polym. Bull. (Berlin)* **1987**, *17*, 465–472.
- (10) Maeda, H. *J. Polym. Sci., Part B: Polym. Phys.* **1994**, *32*, 4299–4301.
- (11) Meeussen, F.; Bauwens, Y.; Moerkerke, R.; Nies, E.; Berghmans, H. *Polymer* **2000**, *41*, 3737–3743.
- (12) Spěváček, J.; Hanyková, L.; Ilavský, M. *Macromol. Symp.* **2001**, *166*, 231–236.
- (13) Maeda, Y. *Langmuir* **2001**, *17*, 1737–1742.
- (14) Yang, Y.; Zeng, F.; Xie, X.; Tong, Z.; Liu, X. *Polym. J.* **2001**, *33*, 399–403.
- (15) Hanyková, L.; Spěváček, J.; Ilavský, M. *Polymer* **2001**, *42*, 8607–8612.
- (16) Spěváček, J.; Hanyková, L. *Macromol. Symp.* **2003**, *203*, 229–237.
- (17) Moerkerke, R.; Meeussen, F.; Koningsveld, R.; Berghmans, H.; Mondelaers, W.; Schacht, E.; Dušek, K.; Šolc, K. *Macromolecules* **1998**, *31*, 2223–2229.
- (18) Arndt, K.-F.; Schmidt, T.; Menge, H. *Macromol. Symp.* **2001**, *164*, 313–322.
- (19) Arndt, K.-F.; Schmidt, T.; Reichelt, R. *Polymer* **2001**, *42*, 6785–6791.
- (20) Starovoytova, L.; Spěváček, J.; Hanyková, L.; Ilavský, M. *Macromol. Symp.* **2003**, *203*, 239–246.
- (21) Starovoytova, L.; Spěváček, J.; Hanyková, L.; Ilavský, M. *Polymer* **2004**, *45*, 5905–5911.
- (22) Salmerón Sánchez, M.; Hanyková, L.; Ilavský, M.; Monleón Pradas, M. *Polymer* **2004**, *45*, 4087–4094.
- (23) Farrar, T. C.; Becker, E. D. *Pulse and Fourier Transform NMR*; Academic Press: New York, 1971; pp 27–29.
- (24) Bauer, C.; Freeman, R.; Frenkel, T.; Keeler, J.; Shaka, A. J. *J. Magn. Reson.* **1984**, *58*, 442–457.
- (25) Bovey, F. A.; Anderson, E. W.; Douglass, D. C.; Manson, J. A. *J. Chem. Phys.* **1963**, *39*, 1199–1202.
- (26) Ramey, K. C.; Field, N. D.; Hasegawa, I. *J. Polym. Sci., Part B: Polym. Lett.* **1964**, *2*, 865–868.
- (27) Abe, A. *Macromolecules* **1977**, *10*, 34–43.
- (28) Morii, H.; Fujiwara, Y.; Matsuzaki, K. *Macromolecules* **1983**, *16*, 1220–1228.
- (29) Matsuzaki, K.; Uryu, T.; Asakura, T. *NMR Spectroscopy and Stereoregularity of Polymers*; Japan Scientific Societies Press: Tokyo, 1996; p 106.
- (30) Yoshino, T.; Shinomya, M.; Komiyama, J. *J. Am. Chem. Soc.* **1965**, *87*, 387–389.
- (31) Schilling, F. C.; Bovey, F. A.; Bruch, M. D.; Kozlowski, S. A. *Macromolecules* **1985**, *18*, 1418–1422.
- (32) Lee, M.-J.; Green, M. M.; Mikeš, F.; Morawetz, H. *Macromolecules* **2002**, *35*, 4216–4217.

- (33) Starovoytova, L.; Spěvák, J.; Ilavský, M. *Polymer*, submitted for publication.
- (34) Spěvák, J.; Hanyková, L.; Ilavský, M. *Macromol. Chem. Phys.* **2001**, *202*, 1122–1129.
- (35) Mao, S.-Z.; Zhang, X.-D.; Dereppe, J.-M.; Du, Y.-R. *Colloid Polym. Sci.* **2000**, *278*, 264–269.
- (36) Ruytinx, B.; Berghmans, H.; Adriaenssens, P.; Storme, L.; Vanderzande, D.; Gelan, J.; Paoletti, S. *Macromolecules* **2001**, *34*, 522–528.
- (37) Valensin, G.; Kushnir, T.; Navon, G. *J. Magn. Reson.* **1982**, *46*, 23–29.
- (38) Spěvák, J.; Suchopárek, M. *Macromol. Symp.* **1997**, *114*, 23–34.
- (39) Spěvák, J.; Suchopárek, M. *Macromolecules* **1997**, *30*, 2178–2181.
- (40) Saiani, A.; Spěvák, J.; Guenet, J.-M. *Macromolecules* **1998**, *31*, 703–710.
- (41) Spěvák, J.; Suchopárek, M.; Mijangos, C.; Lopez, D. *Macromol. Chem. Phys.* **1998**, *199*, 1233–1239.
- (42) Spěvák, J.; Brus, J. *Macromol. Symp.* **1999**, *138*, 117–122.
- (43) Ohta, H.; Ando, I.; Fujishige, S.; Kubota, K. *J. Polym. Sci., Part B: Polym. Phys.* **1991**, *29*, 963–968.
- (44) Starovoytova, L., unpublished results.

MA0486647